CrystEngComm

RSCPublishing

ARTICLE

Engineering Short, Strong Hydrogen Bonds in Urea Di-carboxylic Acid Complexes

Cite this: DOI: 10.1039/x0xx00000x

Andrew O. F. Jones,[a,b,c] Charlotte K. Leech,[d] Garry J. McIntyre,[e] Chick C. Wilson[a], and Lynne H. Thomas[a,*]

Received 00th January 2012,
Accepted 00th January 2012

DOI: 10.1039/x0xx00000x

www.rsc.org/

A series of seven 2:1 molecular complexes of urea (U) and methyl ureas with di-carboxylic acids (A) are reported, along with the results of their study by variable temperature diffraction. These all contain short, strong O-H···O hydrogen bonds and a recurring acid··amide heterodimer forming U-A-U synthons. Despite differences in the degree of saturation of the linking C-C groups of the di-carboxylic acids and the single or double methyl substitution of one of the N atoms of the urea, the packing arrangements are remarkably similar in five of the complexes; the exceptions being *N*-methylurea oxalic acid and *N,N*-dimethylurea fumaric acid. The five similar molecular complexes all show contraction of one unit cell parameter on increasing temperature due to rearrangements of the weaker interactions which hold together the U-A-U units. The strength of the short, strong O-H···O hydrogen bond is shown to be linked both to the length of the connecting bridge between the carboxylic acid groups of the acid, and to the ΔpK_a values between the two components.

Introduction

Hydrogen bonds (HBs) are often the primary intermolecular interaction determining how molecules come together to form a solid and so play a key role in determining the characteristics of many biological, organic and inorganic systems.[1] A detailed understanding of the role of these important interactions is therefore necessary in determining their role in governing the physical properties of a diverse range of materials. Single crystal X-ray diffraction experiments now routinely allow the positional and isotropic thermal parameters of hydrogen atoms to be refined, allowing closer examination of HB networks, although there is often an inherent ambiguity associated with their location. Single crystal neutron diffraction, on the other hand, allows hydrogen atoms to be located unambiguously and both positions and anisotropic displacement parameters can be refined; this is therefore the ideal technique for studying the subtle behaviour of hydrogen atoms.

In some cases, hydrogen atoms display unusual, dynamic behaviour (e.g. disorder[2,3,4] or migration[5-10] across HBs). The information about such atoms extracted from X-ray data alone can be ambiguous due to the inherent inaccuracies in hydrogen atom location from this technique; we have recently demonstrated, however, that utilisation of Fourier difference maps from X-ray diffraction data can reliably identify and characterise these types of effects.[4,10,12] Utilising both X-ray and neutron diffraction in tandem allows comparison of the electronic and nuclear behaviours of the hydrogen atoms, which can provide further insight into the nature of a HB, as the two do not always follow the same pattern of behaviour.[11]

Variable temperature methods can be utilised in diffraction experiments to probe a wide variety of interesting physical and chemical properties including, but not limited to, phase transitions,[13] thermochromism[9] and negative thermal expansion.[14] Subtle temperature-dependent proton effects such as disorder and migration within HBs may be observed and characterised using variable temperature X-ray and neutron studies. With temperature being an easily controllable external variable, it opens up the possibility of crystal structures being "tuned" to display specific structural features. This can aid in the understanding of the processes involved as well as creating materials with potentially useful properties.

Cocrystallisation is another valuable tool when looking to control the properties of compounds in the solid-state. This method is often of particular interest in the pharmaceutical industry where a common problem for active pharmaceutical ingredients (APIs) is low solubility, affecting the bioavailability of a drug in the body. Cocrystallisation enables properties such as solubility to be modified by introducing another compound into the same crystal matrix as the API of interest.[15] Cocrystallisation also allows an extra element of control over the crystal form by, for example, introducing compounds with specific functional groups (acting as HB donors/acceptors) or bulky groups (steric effects) to influence the architecture of the crystal structure which is formed.[16] Whilst it is common to direct the formation of specific hydrogen bonds using crystal

engineering techniques, it is far more difficult to control the strength of these hydrogen bonds. Such precise control is desirable where interesting behaviour within HBs occurs and this can be used as a means of introducing, for example, hydrogen migration leading to thermochromism.[9] Certain categories of HBs offer an increased likelihood of displaying such desirable features; temperature-dependent proton migration in short, strong HBs (SSHBs), for example, tends to require an O-H···O HB of <2.50 Å in length.[10] The proton affinity of the components used in a cocrystallisation experiment can also be harnessed. For example, a correlation between ΔpK_a values and the magnitude of proton migration observed over a given temperature range in SSHBs showed that complexes with the least negative ΔpK_a values displayed the most significant migration.[10]

Urea has been used extensively as a co-molecule in the crystal engineering of molecular complexes due to the presence of multiple HB donor and acceptor sites.[17] It can produce robust and reproducible crystallographic motifs when crystallised with organic acids.[18] Urea di-carboxylic acid complexes often form hydrogen bonded chains with a motif that is dependent on the stoichiometry of the component molecules. 1:1 complexes show a urea (U) - acid (A) motif while 2:1 (urea:acid) and 1:2 complexes show U-A-U and A-U-A motifs, respectively. 1:1 and 2:1 complexes are most common, however there is one example of a 1:2 complex formed by urea and maleic acid.[17] The reliability and predictability of these motifs in urea-acid complexes makes these ideal systems for studying the effect of systematically modifying the substituent on the urea moiety (and therefore the pK_a) on the detailed characteristics of the HBs.

Modification of the substituents of co-molecules can also have a significant impact on the crystallographic motif displayed in a structure; this is often related to the addition or removal of hydrogen bonding sites which will therefore impact the crystal packing.[19] Here, the effect of modifying the urea molecules through the systematic addition of methyl groups to the urea nitrogen atoms, resulting in the blocking of HB donor sites, is of interest. In contrast to the parent urea itself, the *N*-methyl substituted ureas are not well studied, with only one current example of a complex of an organic di-carboxylic acid with a mono-substituted urea; the 2:1 complex of *N*-methylurea (MU) and oxalic acid.[20] The molecular complexes of urea, MU and *N,N*-dimethylurea (DMU) with the di-carboxylic acids fumaric and succinic acid, and of MU with oxalic acid, are reported here, allowing a systematic investigation of the effects of methyl substitutions on the urea on the crystal packing of the complexes (Fig. 1). In addition, the effect of chain length and molecular flexibility on the crystal packing is investigated and variable temperature methods are utilised to follow the structural evolution of the synthesised complexes. Three of the complexes reported here (urea succinic acid,[18,21,22] urea fumaric acid,[22,23] and *N*-methylurea oxalic acid[20]) have been previously studied by X-ray diffraction at room temperature (RT).

Experimental

Crystals of **US** [bis(urea) succinic acid] were obtained by slow evaporation of solvent from an ethanol/DMF mixture at 50°C. Crystals of **UF** [bis(urea) fumaric acid], **MUS** [bis(*N*-methylurea) succinic acid], **MUOX** [bis(*N*-methylurea) oxalic acid], **DMUS** [bis(*N,N*-dimethylurea) succinic acid], and **DMUF** [bis(*N,N*-dimethylurea) fumaric acid] were obtained by slow evaporation of an ethanol solution at RT. Crystals of **MUF** [bis(*N*-methylurea) fumaric acid) were obtained by slow evaporation of solvent from an isopropanol solution at RT.

All X-ray data for **US**, **UF**, **MUS**, **MUF**, **DMUS** and **DMUF** were collected at 100, 200 and 300 K, and at 200 and 300 K for **MUOX,** on a Rigaku R-AXIS/RAPID image plate diffractometer equipped with an Oxford cryosystems N_2 low temperature device[24] using graphite monochromated Mo Kα radiation (λ = 0.71073 Å). Reflections were processed using FSPROCESS within the CRYSTALCLEAR[25] suite of programs and an absorption correction based on the multi-scan method was applied. The structures were solved by direct methods using SHELXS-97[26] and refined with anisotropic displacement parameters for all non-H atoms using SHELXL-97[26] within WinGX.[27] Hydrogen atoms were located using Fourier difference methods and refined isotropically.

Neutron data for **US**, **MUS** and **DMUS** were collected on the Very Intense Vertical Axis Laue Diffractometer (VIVALDI)[28] at the Institut Laue-Langevin reactor source in Grenoble, France. Data were collected at 100, 200 and 300 K for **US**; 20, 100, 200 and 300 K for **MUS** and 20 and 50 K for **DMUS**. No absorption corrections were deemed necessary due to the small size of the crystals used. Orientation matrices were determined using the program LAUEGEN.[29] Unit cell parameters were assumed to be the same as those determined from X-ray data as the Laue method at a continuous neutron source only allows relative linear cell dimensions to be determined. Where there were no X-ray available for the measurements at 20K, the unit cell parameters were first estimated based on the changes in cell dimensions at higher temperatures and then refined to match the data. Reflections were corrected for background and integrated using ARGONNE_BOXES[30] and normalised to a common wavelength, scaled, and merged with LAUE4.[31]

Neutron data for **UF** were collected at 30, 100, 200 and 300 K on SXD,[32] the single crystal diffractometer at ISIS, UK using the time-of-flight Laue diffraction method. The unit cell was refined for each data frame taking the X-ray unit cell as the starting point and an average of these was taken as the unit cell parameters at each temperature. The data were processed using SXD2001.[32]

All neutron data sets were refined using SHELXL-97[26] within the program WinGX[27] with initial atomic coordinates taken from the X-ray structures. All hydrogen positional and anisotropic displacement parameters were refined for each neutron structure.

A summary of the crystallographic data is given in the ESI.†

Table 1: Unit cell and hydrogen bond parameters for all complexes from the 200 K X-ray data.

	Space group	a/Å	b/Å	c/Å	β/°	V/Å^3	O-H···O HB			N-H···O HB		
							D···A	D-H	H···A	D···A	D-H	H···A
US	$P2_1/c$	5.6706(5)	8.1227(7)	12.2182(10)	96.375(3)	559.30(8)	2.521(1)	0.99(2)	1.54(2)	2.966(2)	0.88(2)	2.10(2)
UF	$P2_1/c$	5.671(4)	7.888(5)	12.348(10)	96.719(3)	548.6(15)	2.495(2)	1.03(2)	1.48(2)	2.944(2)	0.89(2)	2.07(2)
MUS	$P2_1/n$	8.2868(7)	5.6618(3)	13.7761(11)	102.959(7)	646.03(8)	2.549(1)	0.93(2)	1.64(2)	2.976(2)	0.91(2)	2.09(2)
MUF	$P2_1/n$	8.551(2)	5.5691(8)	13.909(2)	102.959(7)	645.5(2)	2.533(1)	1.03(2)	1.52(2)	2.933(2)	0.8(2)	2.06(2)
MUOX	$P2_1/c$	5.1081(8)	10.5388(14)	10.2233(14)	102.717(7)	536.85(13)	2.458(2)	1.06(3)	1.43(3)	2.992(3)	0.91(3)	2.10(2)
DMUS	$P2_1/c$	8.6629(12)	5.6284(6)	15.152(2)	100.948(4)	725.3(2)	2.518(1)	0.96(2)	1.57(2)	2.956(1)	0.91(2)	2.05(2)
DMUF	$P2_1/n$	5.8640(5)	18.2369(11)	6.8458(4)	101.330(3)	717.83(9)	2.500(2)	1.02(2)	1.50(2)	2.977(2)	0.85(2)	2.14(2)

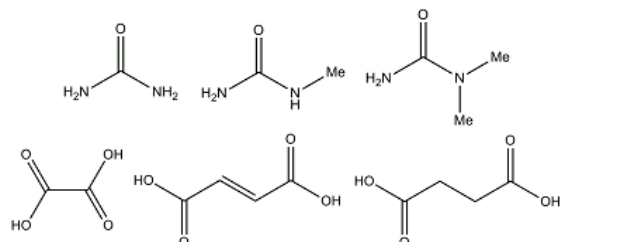

Figure 1. Clockwise from top left, molecular structure diagrams of: urea, N-methylurea, N,N-dimethylurea, succinic acid, fumaric acid and oxalic acid.

Results and Discussion

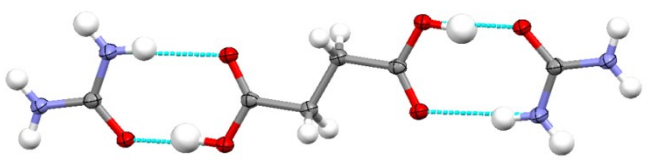

Figure 2. Hydrogen bonded three molecule U-A-U unit in the 100 K X-ray structure of **US**.

Complexes of urea succinic acid (**US**), urea fumaric acid (**UF**), MU succinic acid (**MUS**), MU fumaric acid (**MUF**), MU oxalic acid (**MUOX**), DMU succinic acid (**DMUS**), and DMU fumaric acid (**DMUF**) all crystallise in a 2:1 (urea:acid) ratio and contain a three molecule building block with a U-A-U motif (Fig. 2); this is consistent with those observed by Alhalaweh *et al.*[18] in their studies of urea di-carboxylic acid complexes. The acid···amide homodimer is predicted from computational studies to be one of the most stable hydrogen bonded motifs in these types of complexes.[33] Each structure has one urea molecule and half an acid molecule in the asymmetric unit and all crystallise in space group number 14 (either $P2_1/c$ or $P2_1/n$). The structures of **US**,[18,21,22] **UF**[22,23] and **MUOX**[20] have been previously determined using X-ray diffraction at RT. **US** and **MUOX** both have 1:1 and 2:1 forms with only the 2:1 form of each presented here. The parameters derived for **US/UF/MUOX** in this work are in good agreement with the previously determined structures.

The **US/UF/MUS/MUF** complexes are isostructural; **DMUS** is remarkably similar but with weaker C-H···O HBs replacing N-H···O HBs in connecting the U-A-U motifs into chains. The two other complexes (**MUOX** and **DMUF**) display significantly different motifs.

Structural Similarities

The two pairs of succinic acid and fumaric acid with ureas, **US/UF** and **MUS/MUF**, are isostructural despite the differences in rigidity of the connecting group between the two acid groups and the mono-methyl substitution of the urea moiety (Fig. 3) (Table 1). One-dimensional zigzag chains with a repeating U-A-U motif form and are held together by two $R_2^2(8)$ hydrogen bonded rings; one an amide···amide homodimer and the other an acid···amide heterodimer containing a short, strong O-H···O HB (Fig. 4, left). The addition of a methyl group to the urea molecule in the *anti* conformation (with the methyl group located on the opposite side of the molecule from the carbonyl group) does not perturb the formation of one-dimensional MU-A-MU zigzag chains. Each chain is surrounded by neighbouring chains in a different orientation; the urea complexes show a slightly lower tilt angle between neighbouring chains (66 - 72° over the 100 – 300 K temperature range measured; estimated from the angle between the planes of the acid molecules in each chain) compared to that in the *N*-methylurea complexes (71 - 79°). Chains in the same orientation are stacked on top of one another; the chains in the *N*-methyl urea complexes are spaced more widely to accommodate the methyl groups which point along the *c*-axis (~3.0 - 3.3 Å between layers for **US/UF**; 3.2 - 3.5 Å for **MUS/MUF**) (Fig. 4, right). The motif of alternating chain orientations repeats along the *c*-axis and adjacent chains are held in place by lateral N-H···O HBs between the urea and acid molecules in the different chains forming a complex three-dimensional hydrogen bonded network (Fig. 4, right). The presence of methyl groups in **MUS/MUF** leads to additional

weaker C-H···O HBs between the methyl groups and acid oxygen atoms of different chains.

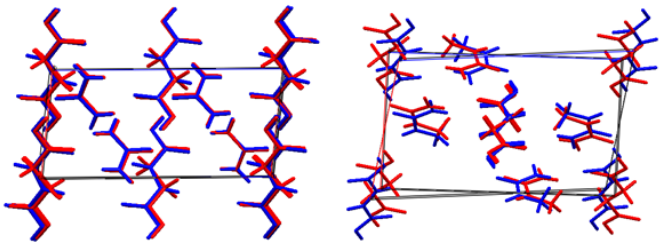

Figure 3: Structural overlay of unit cells of the **US** (red) and **UF** (blue) complexes (left) and the **MUS** (red) and **MUF** (blue) complexes (right) looking along the b-axes, from the 100 K X-ray structures.

The fact that the **US** and **UF** (or **MUS** and **MUF**) complexes are isostructural is not unexpected, given that the only difference between the two is the degree of saturation of the C-C bond at the centre of the acid molecule (Fig. 3). In **US**, where the C-C bond at the centre of the acid molecule is saturated, the presence of additional hydrogen atoms on the alkyl chain results in a larger separation between chains compared to **UF**; at higher temperatures the difference is much smaller (~3.25 (100 K) and ~3.32 Å (300 K) in **US**; ~2.99 (100 K) and ~3.29 Å (300 K) in **UF** (X-ray data)); this also contributes towards a larger cell volume for **US** compared with that of **UF** at all temperatures (Table 3). Other contributions to the difference in volume arise from the shorter U-A-U unit in **UF**, arising from the C=C bond, and also from the HBs in the homo- and heterodimers which are longer in **US**.

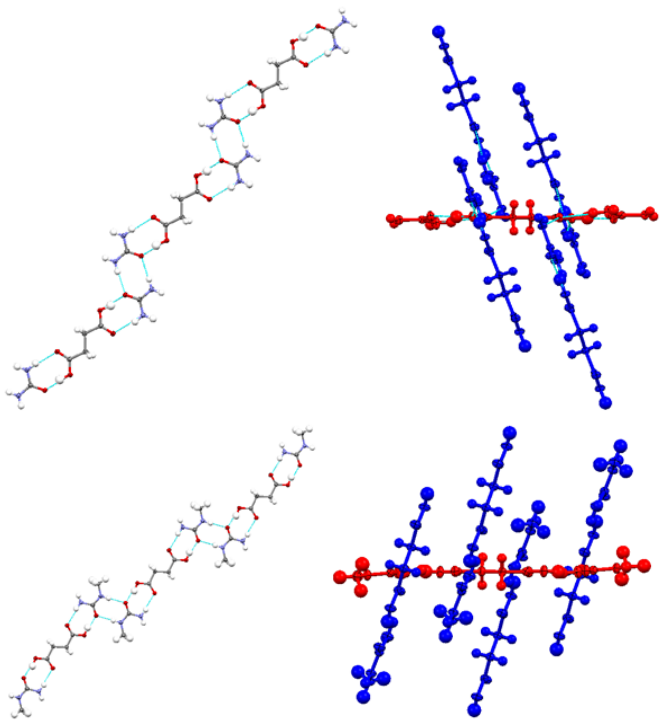

Figure 4: One-dimensional zigzag molecular chain (left; top **US**, bottom **MUS**) and the two possible orientations of chains (right, red and blue; top **US**, bottom **MUS**) in the 100 K X-ray structures of **US** and **MUS**.

A similar observation is found in the structures of the **MUS** and **MUF** complexes (again the only difference is the saturation of the C-C bond) where the layer separation is ~3.43 (100 K) and ~3.51 Å (300 K) in **MUS** and ~3.30 (100 K) and ~3.42 Å (300 K) in **MUF** (X-ray data) (Fig. 4, right). The majority of HBs are longer in **MUS**, contributing again to an increase in volume; the N-H···O HB linking the amide···amide dimers is an exception. The C-C bond in **MUS** leads to longer MU-A-MU units which also contribute to the difference in volume when compared with **MUF**.

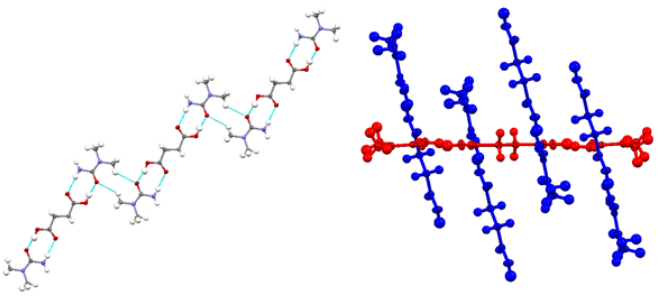

Figure 5: One-dimensional zigzag chain (left) and the two possible orientations of chains (right, red and blue) in the 100 K X-ray structure of **DMUS**.

DMUS and **DMUF** have two methyl groups located on the same nitrogen atom in the urea moiety meaning that the one-dimensional zigzag chains observed in **US**/**UF**/**MUS**/**MUF** cannot form in the same way and the amide···amide homodimers linking adjacent chains are lost. The structure of **DMUS** is, however, remarkably similar to those of **US**/**UF**/**MUS**/**MUF** despite this, as a one-dimensional chain can be formed by utilising two weaker C-H···O interactions between two DMU molecules as opposed to the two symmetric N-H···O HBs in **US**/**UF**/**MUS**/**MUF** (Fig. 5, left); this is unexpected. This causes a shift in the relative positions of neighbouring DMU-A-DMU units, though the interactions between chains in different orientations remain similar to those in **MUS** and **MUF**. The three molecule DMU-A-DMU units again contain $R_2^2(8)$ hydrogen bonded rings made up of a short, strong O-H···O HB and an N-H···O HB. Adjacent chains in different orientations are aligned along the *c*-axis, tilted at 74 - 78° to each other (estimated by the angle between the planes formed by the acid molecules) and are held in place by lateral N-H···O HBs and weaker C-H···O interactions as in **MUS** and **MUF** (Fig. 5, right). Chains in the same orientation form layers with a separation of ~3.3 - 3.5 Å. The increase in the length of the *c*-axis can be related to the increased size of the methyl groups causing an increase in the separation of adjacent chains primarily in the *c* direction (Table 3). The formation of chains similar to those in the **US**/**UF**/**MUS**/**MUF** complexes through different interactions indicates the remarkable stability of this packing motif even when the possibility of linking the urea moieties through an N-H···O HB is removed.

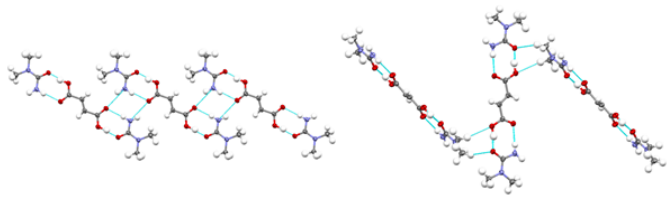

Figure 6: One-dimensional chain of molecules (left) and interactions between chains in different orientations (right) in the 100 K X-ray structure of **DMUF**.

It might be expected that **DMUS** and **DMUF** would pack in a similar manner, but the data presented here do not support this. The structure of **DMUF** contains DMU-A-DMU units containing $R_2^2(8)$ hydrogen bonded rings made up of a short, strong O-H···O HB and an N-H···O HB, similar to the other structures presented here. This structure contrasts with that of **DMUS** as DMU-A-DMU units form into one-dimensional chains through an $R_2^4(8)$ hydrogen bonded ring between an amide group and the carbonyl oxygen atoms of two neighbouring units, including bifurcated HBs formed by the carbonyl oxygen atoms acting as hydrogen bond acceptors from two DMU moieties (Fig. 6, left); this represents a shift in the relative DMU-A-DMU units by approximately the length of a DMU molecule compared to the other complexes and results in a more ribbon-like chain. These interactions between the DMU-A-DMU units to form chains are stronger than those observed in **DMUS** where one of the N-H···O hydrogen bonds is replaced by a weaker C-H···O hydrogen bond. Adjacent chains in different orientations are aligned along the *b*-axis and held in place by weak C-H···O interactions between the DMU and the hydroxyl oxygen of a fumaric acid molecule (Fig. 6, right) which is similar to those seen in the **US/UF/MUS/MUF/DMUS** structures. The angle between the planes of the acid molecules in the two different chains is ~86°. Chains in the same orientations are again layered with an approximate spacing of 3.2 - 3.4 Å.

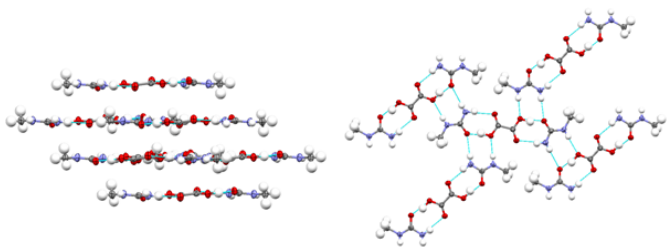

Figure 7: The layered structure (left) and hydrogen bonds between three molecule units in a layer (right), from the 200 K X-ray structure of **MUOX**.

The 2:1 form of **MUOX** packs in a different manner to the other structures.[20] Oxalic acid has a shorter alkyl chain than both fumaric and succinic acid but it can still pack in a similar manner evinced by a complex of the DMU isomer *N,N'*-dimethylurea (N,N'DMU; the urea is disubstituted with methyl groups but this time on different N atoms) and oxalic acid; the N,N'DMU molecules arrange in U-A-U units although the packing of these differs from **US/UF/MUS/MUF/DMUS**.[10] However, in the present study, MU does not form this motif with oxalic acid and instead forms a layered structure (Fig. 7, left). This type of layered packing has been observed for DMU oxalic acid[10] and urea succinic acid.[18] The original structural determination of **MUOX**, reports a phase transition to orthorhombic symmetry occurring at ~180 K as the temperature is decreased. A data collection was thus attempted at 100 K, but the phase transition resulted in a decrease in the quality of the crystal and a stable refinement could not be obtained; therefore only 200 and 300 K X-ray structures were determined. The MU molecule in **MUOX** is in the *syn* conformation as opposed to *anti* in **MUS** and **MUF**, with the methyl group on the same side of the molecule as the carbonyl group meaning that zigzag chains cannot form and the amide···amide homodimer linking the three molecule units is lost. Adjacent MU-A-MU units are no longer parallel in their arrangement into chains; instead every second unit is parallel and the structure is layered. Adjacent units are held in place by $R_3^2(8)$ hydrogen bonded rings forming between two MU molecules and an acid to produce a two-dimensional hydrogen bonded network (Fig. 7, right). These hydrogen bonded rings are made up of one moderate and one weak N-H···O HB and a strong O-H···O HB in the three molecule unit. The layer separation is ~3.0 Å with $\pi - \pi$ interactions between the carbonyls of the acid and MU in different layers.

Short, Strong Hydrogen Bonds

The seven molecular complexes in this work contain O-H···O HBs of lengths in the range 2.45 – 2.55 Å (depending on the complex and the temperature of structural determination, Table 2). In general, the smaller the linking di-carboxylic acid, the shorter the HB and this is independent of the urea derivative. The effect of urea substituent on the HB length for a given di-carboxylic acid is, however, more subtle.

Previously a correlation between ΔpK_a values and the length of SSHB has been identified.[10] All complexes reported here have negative ΔpK_a values, indicating that neutral co-crystal formation should be expected. The least negative value occurs for **MUOX**, which also shows the shortest O-H···O distance. Compared to the previously reported DMU and *N,N'*-dimethylurea oxalic complexes,[10] **MUOX** has a longer O-H···O distance despite having a ΔpK_a value in between the two (it would be expected, by this argument, to have a shorter O-H···O HB than the **NN'DMUOX** structure). This demonstrates the importance of the local environment and the additional intermolecular interactions to the HB; **MUOX** displays a significantly different packing arrangement compared to the other complexes. As the ΔpK_a values become increasingly negative there is a general trend for an increasing O-H···O distance. Despite the difficulties in transferring pK_a values to the solid-state, the fact that they tend to be determined using water as the solvent, and the question of how appropriate they may be for complexes which do not display a 1:1 stoichiometry, this general trend demonstrates that there is clear potential for ΔpK_a values to be used as a tool to tune the HB strength in complexes which contain a SSHB (by choosing

related molecules with suitable pK_a values) and thus any potentially interesting properties that may arise from such HBs.

Table 2: ΔpK_a values and O-H···O HB distances from the 300 K X-ray data for the seven complexes.

Complex	ΔpK_a	r(O-H···O) / Å
DMUOX[10]	-1.56	2.439(2)
MUOX	-1.57	2.461(2)
NN'DMUOX[10]	-1.94	2.4548(12)
UF	-3.05	2.498(2)
DMUF	-3.33	2.501(2)
MUF	-3.34	2.536(2)
US	-4.14	2.5298(15)
DMUS	-4.42	2.5234(15)
MUS	-4.43	2.553(2)

NN'DMUOX = *N,N'*-dimethylurea oxalic acid 2:1 complex

The phenomenon of proton migration in SSHBs is rare, but a link between the O-H···O HB length and the occurrence of migration has been suggested; migration tends to occur only in O-H···O HBs less than 2.45 Å in length (O···O distance).[10] In order to investigate the possibility of proton migration in the current materials, variable temperature neutron studies have been carried out on **US**/**UF**/**MUS**/**DMUS**. No evidence of temperature dependent proton migration was found within the complexes, suggesting that the proposed HB length threshold of ≤2.45 Å remains a sensible one (see ESI†). **MUOX** is the complex containing the shortest HB of the seven complexes, however, it was not possible to grow crystals of a suitable size for neutron diffraction studies. Whilst the X-ray data do not give any indication of proton migration, with this complex containing a SSHB of a length near the proposed threshold value, it is a sensible candidate for future neutron experiments.

Temperature Dependent Effects

Variable temperature experiments reveal another interesting feature of some of the complexes presented here, which can be related to the crystal packing. As the temperature is increased, the unit cell volume of a material will generally increase due to the increased thermal motion of the atoms and molecules within. In the solid-state, the expansion is often not uniform in all directions due to the alignment of molecules within the structure making expansion anisotropic – more favourable in certain directions – causing some axes or angles to increase at a different rate to others. **US**/**UF**/**MUS**/**MUF**/**DMUS**, which have very similar packing motifs, display the unusual property of contraction in one of the unit cell axes on increasing the temperature (Table 3). In all of these complexes, the contraction of the unit cell axis is accompanied by an increase in the unit cell volume, so these complexes cannot be called negative thermal expansion materials. **MUOX** and **DMUF** have different packing motifs and do not display this thermal expansion property.

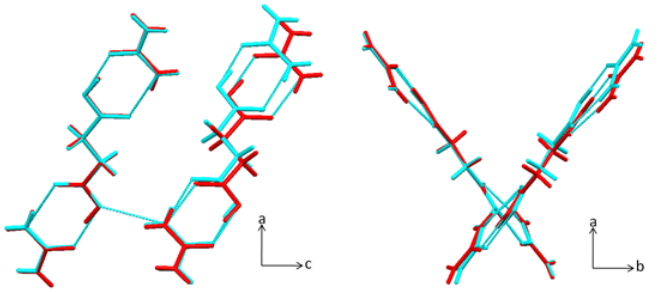

Figure 8: Structural overlay of **US** at 100 (cyan) and 300 K (red) viewed along the b- (left) and c-axes (right), taken from the X-ray structure determinations.

The contraction of a single unit cell axis can be rationalised by a shift in the hydrogen bonded molecular units as the temperature is increased (Fig. 8). Several factors contribute to this; increased thermal motion can have a pronounced effect on HB distances as these are weaker and more flexible than covalent bonds and can increase with temperature. This effect might be expected to be less pronounced for the short, strong O-H···O HBs in these complexes as these interactions are more covalent in nature. In the three molecule U-A-U unit of **US** the O-H···O distance increases from 2.515(1) to 2.530(2) Å and the N-H···O distance increases from 2.947(1) to 2.988(2) Å at 100 and 300 K, respectively (X-ray data). In **US**/**MUS**/**MUF**, both of these HB distances in the same molecular units increase, while **UF** shows only the N-H···O distance increasing, with the O-H···O distance being invariant over the temperature range. In **DMUS**, both distances are invariant. The lateral HBs from the three molecule units to neighbouring chains increase in length with temperature in all of the complexes. The cooperative effect of these increases in hydrogen bond lengths with temperature results in a shifting of the relative positions of the molecular units and results in associated compression of weaker intermolecular interactions; it is the compression of these interactions that gives rise to the contraction in one cell dimension.

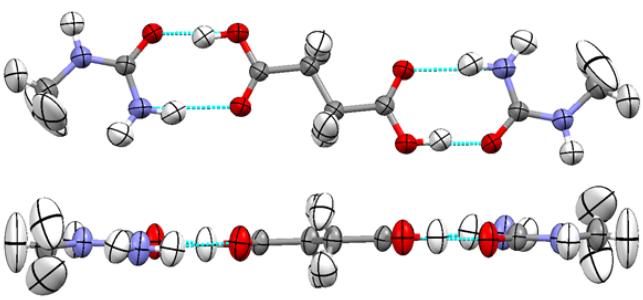

Figure 9: A molecular unit viewed from above (top) and the side (bottom) showing the large anisotropic thermal parameters of the hydrogen atoms indicative of libration in the case of the methyl groups in the 300 K neutron structure of **MUS**.

Table 3: Unit cell parameters of selected complexes from the 100 and 300 K X-ray data with contracting unit cell axes shown in bold.

	a / Å	*b* / Å	*c* / Å	*β* / °	V / Å^3
US 100K	**5.7109(7)**	7.9698(11)	12.1580(15)	96.160(4)	550.17(3)
US 300K	**5.6366(6)**	8.2568(10)	12.2790(13)	96.659(4)	567.61(3)
UF 100K	**5.764(2)**	7.640(2)	12.283(4)	96.901(11)	537.0(3)
UF 300K	**5.541(6)**	8.214(7)	12.427(12)	97.314(8)	561.0(2)
MUS 100K	8.0244(12)	**5.7496(7)**	13.735(2)	91.246(5)	633.54(2)
MUS 300K	8.5398(8)	**5.5798(4)**	13.8377(16)	92.291(4)	658.84(2)
MUF 100K	8.2188(10)	**5.6497(5)**	13.8382(13)	104.156(4)	630.63(7)
MUF 300K	8.7741(14)	**5.4413(7)**	13.9303(19)	100.730(6)	653.44(8)
DMUS 100K	8.483(3)	5.5169(14)	**15.415(5)**	101.677(8)	706.49(13)
DMUS 300K	8.797(2)	5.6934(13)	**15.059(4)**	100.764(7)	740.96(11)

Increased thermal motion within the crystal structures at higher temperatures results in the atomic displacement parameters increasing in size; this is particularly the case for the hydrogen atoms (Fig. 9). In **US**/**UF**/**MUS**, where neutron data are available at 300 K, the anisotropic thermal parameters of the hydrogen atoms can be refined and the direction of largest motion established. The hydrogen atoms with the largest displacement parameters, as might be expected, are those located on the alkyl chains of the fumaric and succinic acid molecules, which are not involved in any HBs, and those located on methyl groups of the substituted ureas in **MUS** where there is significant libration of the methyl groups at higher temperatures.[35] Hydrogen atoms located on the amide groups of the ureas (and the nitrogen atoms themselves) also show motion out of the plane of the molecular unit (indicated as a large principal mean square atomic displacement parameter in this direction) due to a 'wagging' of the amide group. This occurs in part due to the amide group only being involved in moderate to weak HBs and the thermal displacement parameters for these hydrogen atoms are larger than those involved in the much stronger O-H···O HBs. The motion of these atoms out of the plane of the molecular unit can also be related to a slight increase in the distance between layers of the one-dimensional chains in all of **US**/**UF**/**MUS**/**MUF**/**DMUS**; for example in **US** the layer separation increases from ~3.23 to ~3.30 Å in the 100 and 300 K X-ray structures, respectively. The combination of these factors has the net effect of a contraction of one unit cell axis due to the compression of weaker interactions noted above. This effect is entirely dependent on the crystal packing and the changes that occur in the weak interactions on varying the temperature.

The thermal behaviour exhibited in these complexes is similar to that observed in the complex of *N,N′*-dimethylurea oxalic acid, which also displays a contraction of one unit cell axis on an increase in temperature.[10]

Conclusions

Seven urea and methylurea-dicarboxylic acid complexes have been studied using variable temperature X-ray diffraction while variable temperature neutron data were also collected on four of these complexes. All seven complexes have a 2:1 (urea:acid) stoichiometry and contain a common motif of a three molecule hydrogen bonded U-A-U unit, consistent with the motifs observed in urea di-carboxylic acid complexes by Alhalaweh *et al.*[18] The presence of the acid···amide heterodimer motif persists in all complexes, reflecting the strength of this motif in directing the crystal structure. Modification of the urea moieties involved in these complexes by the addition of methyl groups removes the "competing" amide···amide homodimer preferentially over the acid···amide dimer in structures **MUOX**/**DMUS**/**DMUF**, where it is not possible to maintain both at the same time. This effectively pairs the strongest proton donor groups with the strongest HB acceptors.[34] **US**/**UF**/**MUS**/**MUF**/**DMUS** all display very similar crystal packing motifs with one-dimensional zigzag chains in two orientations where chains in the same orientation are stacked on top of one another. **DMUF** forms a different kind of hydrogen bonded chain, but still has two possible chain orientations and stacking of chains in the same orientation, while **MUOX** has a different packing motif and forms a layered structure.

The similarity of the packing in complexes **US**/**UF**/**MUS**/**MUF**/**DMUS** shows the robustness of the acid···amide heterodimer which is formed preferentially over the amide···amide homodimer when methyl groups are added to the urea moiety in **MUS**, **MUF** and **DMUS**. The similarity of the packing motif in **DMUS** with those of complexes **US**/**UF**/**MUS**/**MUF** was unexpected as the presence of two methyl groups on the urea means that an amide···amide dimer cannot form. However, a one-dimensional chain is formed through two equivalent C-H···O interactions between the methyl groups and carbonyl oxygen atoms of the DMU molecules. This packing motif adds an element of predictability to the structures, potentially enabling complexes containing similar molecules to be designed rationally in the future.

The packing motif in the **US/UF/MUS/MUF/DMUS** complexes leads to unusual temperature dependent behaviour where one unit cell axis contracts on increasing the temperature. The contraction can be rationalised through a shift in the positions of adjacent molecular chains related to the increased thermal motion of the molecules and changes in the HBs and other weaker interactions as the temperature was varied.

Neutron data were collected on four of the complexes to investigate the possible presence of proton migration in the short, strong O-H···O HBs which are present in all of the complexes. None of the complexes showed any significant change in the position of the proton in the SSHB as the temperature was varied. A HB distance of ~2.45 Å has previously been suggested as a threshold, below which proton migration may be observed.[10] The findings reported here support this, as the O···O separations in the SSHB of the four complexes studied by neutron diffraction are all greater than this threshold value. The length of the bridging di-carboxylic acid molecule influences the strength of the O-H···O HB; the shorter the linker, the shorter the HB. A general trend of HB length with ΔpK_a values can be seen although this is more subtle; the less negative the ΔpK_a value, the shorter the HB formed. Other factors such as crystal packing have an effect on the SSHB distance evinced by the anomaly of **MUOX**.

Acknowledgements

We thank the ILL and ISIS for the provision of neutron beam time, and the ILL for studentship funding.

Notes and references

[a] Department of Chemistry, University of Bath, Bath, BA2 7AY, UK. Email: L.H.Thomas@bath.ac.uk.

[b] Institut Laue-Langevin, 38042 Grenoble, France.

[c] Now at Département de Physique, Faculté des Sciences, Université Libre de Bruxelles CP223, Campus de la Plaine, 1050 Brussels, Belgium.

[d] ISIS Facility, STFC Rutherford Appleton Laboratory, Harwell Innovation Campus, Didcot, Oxon OX11 0QX, UK.

[e] Australian Nuclear Science and Technology Organisation, Lucas Heights, NSW 2234, Australia.

† Electronic Supplementary Information (ESI) available: Summary of the crystallographic data, details of the short, strong hydrogen bond lengths, details of the variation of hydrogen bond length with temperature, Fourier difference maps imaging the hydrogen atoms from both X-ray and neutron data, cifs CCDC 992787-992819. See DOI: 10.1039/b000000x/

1 G. R. Desiraju, *Angew. Chem. Int. Ed.* 2011, **50**, 52.

2 C. C. Wilson, N. Shankland, A. J. Florence, *J. Chem. Soc., Faraday Trans.*, 1996, **92**, 5051.

3 A. Parkin, C. C. Seaton, N. Blagden, C. C. Wilson, *Cryst. Growth Des.*, 2007, **7**, 531.

4 A. O. F. Jones, N. Blagden, G. J. McIntyre, A. Parkin, C. C. Seaton, L. H. Thomas, C. C. Wilson, *Cryst. Growth Des.*, 2013, **13**, 497.

5 C. C. Wilson, K. Shankland, N. Shankland, *Z. Kristallogr.*, 2001, **216**, 303.

6 C. C. Wilson, *Acta Cryst.*, 2001, **B57**, 435.

7 J. A. Cowan, J. A. K. Howard, G. J. McIntyre, S. M. F. Lo, I. D. Williams, *Acta Cryst.*, 2003, **B59**, 794.

8 J. A. Cowan, J. A. K. Howard, G. J. McIntyre, S. M. F. Lo, I. D. Williams, *Acta Cryst.*, 2005, **B61**, 724.

9 D. M. S. Martins, D. S. Middlemiss, C. R. Pulham, C. C. Wilson, M. T. Weller, P. F. Henry, N. Shankland, K. Shankland, W. G. Marshall, R. M. Ibberson, K. Knight, S. Moggach, M. Brunelli, C. A. Morrison, *J. Am. Chem. Soc.*, 2009, **131**, 3884.

10 A. O. F. Jones, M.-H. Lemée-Cailleau, D. M. S. Martins, G. J. McIntyre, I. D. H. Oswald, C. R. Pulham, C. K. Spanswick, L. H. Thomas, C. C. Wilson, *Phys. Chem. Chem. Phys.*, 2012, **14**, 13273.

11 L. H. Thomas, A. J. Florence, C. C. Wilson, *New J. Chem.*, 2009, **33**, 2486.

12 S. M. Harte, A. Parkin, A. E. Goeta, C. C. Wilson, *J. Mol. Struct.*, 2005, **741**, 93.

13 P. K. Allan, B. Xiao, S. J. Teat, J. W. Knight, R. E. Morris, *J. Am. Chem. Soc.*, 2010, **132**, 3605.

14 J. S. O. Evans, *J. Chem. Soc., Dalton Trans*, 1999, 3317.

15 P. Vishweshwar, J. A. McMahon, J. A. Bis, M. J.; Zaworotko, *J. Pharm. Sci.*, 2006, **95**, 499.

16 J. M. Kelleher, S. E. Lawrence, H. A. Moynihan, *CrystEngComm* 2006, **8**, 327.

17 V. Videnova-Adrabinska, *J. Mol. Struct.*, 1996, **374**, 199.

18 A. Alhalaweh, S. George, D. Boström, S. P. Velaga, *Cryst. Growth Des.*, 2010, **10**, 4847.

19 J. I. Arenas-García, D. Herrera-Ruiz, K. Mondragón-Vásquez, H. Morales-Rojas, H. Höpfl, *Cryst. Growth Des.*, 2011, **12**, 811.

20 S. Harkema, J. H. M. Ter Brake, H. J. G. Meutstege, *Acta Cryst.*, 1979, **B35**, 2087.

21 H. Wiedenfeld, F. Knoch, *Acta Cryst.*, 1990, **C46**, 1038.

22 V. Videnova-Adrabinska, *Acta Cryst.*, 1996, **B52**, 1048.

23 G. Smith, C. H. L. Kennard, K. A. Byriel, *Aust. J. Chem.*, 1997, **50**, 1021.24.

24 J. Cosier, A. M. Glazer, *J. Appl. Cryst.*, 1986, **19**, 105.

25 CRYSTALCLEAR, Rigaku Corporation, Tokyo, Japan.

26 G. M. Sheldrick, *Acta Crystallogr.*, 2008, **A64**, 112.

27 L. J. Farrugia, *J. Appl. Cryst.*, 1999, **32**, 837.

28 G. J. McIntyre, M.-H. Lemée-Cailleau, C. Wilkinson, *Physica B* 2006, **385-386**, 1055.

29 J. W. Campbell, Q. Hao, M. M. Harding, N. D. Nguti, C. Wilkinson, *J. Appl. Cryst.*, 1998, **31**, 496.

30 C. Wilkinson, H. W. Khamis, R. F. D. Stansfield, G. J. McIntyre, *J. Appl. Cryst.*, 1988, **21**, 471.

31 R. O. Piltz, *Acta Crystallogr.*, 2011, **A67**, C155.

32 D. A. Keen, M. J. Gutmann, C. C. Wilson, *J. Appl. Cryst.*, 2006, **39**, 714.

33 A. J. Cruz-Cabeza, G. M. Day, W. Jones, *Chem. Eur. J.*, 2008, **14**, 8830.

34 M. C. Etter, *Acc. Chem. Res.*, 1990, **23**, 120.

35 C. C. Wilson, *Chem. Phys. Lett.*, 2001, **335**, 57.

